

## Lectin Recognizable Biomaterials Synthesized via Nitroxide-Mediated Polymerization of a Methacryloyl Galactose Monomer

S. R. Simon Ting,<sup>†,‡</sup> Eun Hee Min,<sup>†,‡</sup> Pierre Escalé,<sup>‡</sup> Maud Save,<sup>‡</sup> Laurent Billon,<sup>\*,‡</sup> and Martina H. Stenzel<sup>\*,†</sup>

<sup>†</sup>Centre for Advanced Macromolecular Design, School of Chemical Sciences and Engineering, University of New South Wales, Sydney NSW 2052, Australia, and <sup>‡</sup>IPREM Equipe de Physique et Chimie des Polymères, UMR 5254 CNRS, Université de Pau et des Pays de l'Adour, Hélioparc 2, Avenue du Président Angot, 64053 Pau Cedex, France

Received August 27, 2009; Revised Manuscript Received October 12, 2009

**ABSTRACT:** The preparation of poly(2-(2',3',4',6'-tetra-*O*-acetyl- $\beta$ -D-galactosyloxy)ethyl methacrylate-*co*-styrene) (P(AcGalEMA-*co*-S)) glycopolymer was performed via nitroxide-mediated polymerization using a methacrylic acid-based alkoxyamine with *N*-tert-butyl-*N*-(1-diethylphosphono-2,2-dimethylpropyl) (SG1) nitroxide as mediating agent. In the presence of a low proportion of styrene, the polymerization of the glycomonomer was conducted in a controlled fashion at 85 °C. The synthesis of the diblock copolymers was investigated via two routes by using either P(AcGalEMA-*co*-S) or polystyrene macroinitiators capped with SG1 nitroxide to yield P(AcGalEMA-*co*-S)-*b*-PS and PS-*b*-P(AcGalEMA-*co*-S), respectively. The AcGalEMA moieties on the diblock copolymer were deacetylated to afford carbohydrate-based amphiphilic diblock copolymer, polystyrene-*block*-poly(2-( $\beta$ -D-galactosyloxy)ethyl methacrylate-*co*-styrene) (PS-*b*-P(GalEMA-*co*-S)). The self-assembling properties of PS-*b*-P(GalEMA-*co*-S) amphiphilic diblock copolymers were thoroughly exploited to obtain micellar structures and porous films. Lectin binding assays were conducted using the UV-vis spectroscopy and dynamic light scattering to test the biofunctionality of the  $\beta$ -galactose moieties with peanut agglutinin (PNA) on the micelles. The polymer was used to prepare honeycomb structured porous films with bioactivity. Fluorescent PNA was eventually conjugated with the sugar moieties on the porous films. Most protein was conjugated to glycopolymer inside the pore, demonstrating that this procedure can be a simple route to pattern proteins onto surfaces.

### Introduction

Carbohydrates are recognized today as information-rich biomolecules in the human body. Sugars in biological systems play important roles such as in cell to cell recognition, signal transmission events, and fertilization.<sup>1</sup> These various functions have attracted scientists, in particular polymer chemists, to investigate sugar-based synthetic polymers, glycopolymers, and biologically related molecules such as glycoproteins. Glycopolymers are synthetic polymers that carry pendant carbohydrate moieties.<sup>2</sup> With polymers that have sugar functional groups or carry glycoproteins, polymer chemists or biomedical engineers could eventually mimic biological systems. Biosynthetic materials are proposed for drug delivery,<sup>3</sup> radio-labeled sugar-nucleotide donors,<sup>4,5</sup> and the modifications of surfaces.<sup>6–8</sup> The synthesis of glycopolymers with different architectures is an important avenue toward understanding how these polymers behave. It has been suggested that the polymer architecture has a profound influence on the binding between glycopolymer and specific proteins.<sup>9</sup> The interaction between one sugar molecule and proteins is rather weak, but the simultaneous interaction between multivalent carbohydrates and proteins results in strong binding.<sup>9–17</sup> Significant efforts have been devoted to explore the multivalency effect with spherical structures such as dendrimers

showing superior interaction.<sup>18–21</sup> The recognition of proteins by glycopolymers is not only of interest in solution. Glycopolymers immobilized onto surface could also serve as screening devices.<sup>18</sup> Honeycomb structured porous films, which are prepared via the breath figure method,<sup>22–25</sup> were recently investigated as a scaffold for protein immobilization.<sup>7</sup>

Glycopolymers can be synthesized either by the polymerization of sugar-containing monomers<sup>2,26–34</sup> or by postpolymerization glycosylation reaction.<sup>6,35,36</sup> These two methods provide a vast variety of options in synthesizing glycopolymers. Glycomonomers can be easily synthesized via the acylation or the chemoenzymatic synthesis of carbohydrates.<sup>2,3</sup> Other methods such as an ester formation reaction<sup>32</sup> and conducting reaction at high temperature with ether bond formation were also being carried out.<sup>37</sup> These monomers can be employed in various controlled living polymerizations techniques such as living anionic polymerization,<sup>38</sup> ring-opening metathesis polymerization (ROMP),<sup>39</sup> nitroxide-mediated radical polymerization (NMP),<sup>32,34,40–45</sup> atom transfer radical polymerization (ATRP),<sup>33,46–49</sup> and reversible addition-fragmentation chain-transfer polymerization (RAFT).<sup>3,26–30,37,50–57</sup>

In the present work, we present the polymerization of a sugar-containing methacrylic monomer via nitroxide-mediated controlled free-radical polymerization using a phosphonate-based nitroxide as controlled agent (SG1) and a SG1-based alkoxyamine as initiator (Scheme 1). The use of polymers in biological systems poses an important consideration regarding toxicity, which could result in low cell proliferations. ATRP

\*Corresponding author: Fax +33 05 59 40 76 23, Tel +33 05 59 40 76 09, e-mail laurent.billon@univ-pau.fr (L.B.); Fax +61 2 93854344, Tel +61 2 93856250; e-mail m.stenzel@unsw.edu.au (M.H.S.).

requires the thorough purification of the polymers to avoid the risk of introducing toxic elements such as copper catalyst and amino ligands. Some RAFT generated polymers can potentially be toxic as a result of the presence of thiocarbonyl thio groups.<sup>58</sup> Polymers capped with phosphonate groups in SG1-mediated controlled free-radical polymerization on the other hand provide safer materials when used in biological applications. Toxicity is usually reduced compared to polymers synthesized using RAFT and ATRP as nitroxide compounds have been widely tested to be used as antioxidants and probes for various applications in the biological systems.<sup>59,60</sup>

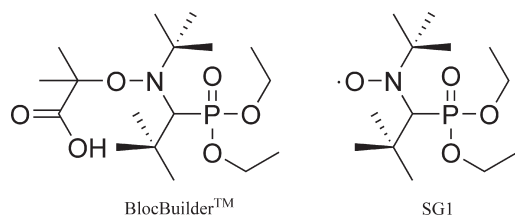
Among the three most common controlled radical polymerization techniques, NMP, ATRP, and RAFT, NMP is the oldest techniques, and yet the synthesis of well-defined glycopolymers has rarely been reported using it. Fukuda and co-workers investigated the polymerization of acrylate and styrenic-based glycomonomers using a di-*tert*-butyl nitroxide (DBN)-based alkoxyamine initiator.<sup>32,34,40</sup> Kakuchi and co-workers also employed 2,2,6,6-tetramethylpiperidinyloxy-terminated polystyrene (PS-TEMPO) macroinitiator to chain extend two styrenic-based glucoside peracetate and maltohexaoside peracetate glycomonomers with a reaction temperature of 138 °C.<sup>44</sup> In addition, Hawker's group reported the polymerization of 1,2,5,6-di-(isopropylidene)-D-glucose-2-propenoate with an  $\alpha$ -hydrido alkoxyamine initiator at a reaction temperature of 105 °C.<sup>41</sup> However, the use of methacrylate-based glycomonomers has not yet been documented via nitroxide-mediated free-radical

polymerization as the control of methacrylic esters homopolymerization via NMP is rather difficult. Indeed, either irreversible disproportionation reactions between the nitroxide and the growing methacrylic radical or high production of macroradicals due to the high value of the activation–deactivation equilibrium constant prevented the synthesis of well-defined methacrylic ester polymers via NMP.<sup>61</sup> More recently, Charleux and co-workers showed that the addition of a very small amount of styrene (less than 10 mol % vs methacrylic ester) was enough to drastically decrease the average activation–deactivation equilibrium constant, hence allowing the controlled polymerization of methyl methacrylate via SG1-mediated polymerization and the preparation of methacrylate-based block copolymers.<sup>62–64</sup> However, the high polymerization temperatures of NMP maybe a concern in the preparation of glycopolymers as the latter become unstable at temperatures higher than 120 °C.<sup>34</sup> In order to overcome the predicament of high-temperature NMP reactions, Charleux et al. performed a controlled free-radical polymerization of methacrylic acid at 73 and 83 °C in the presence of a low concentration of styrene using BlocBuilder alkoxyamine and SG1 nitroxide.<sup>65</sup> This strategy was used in the present work to design new diblock copolymers based on methylacryloyl glycomonomer and styrene.

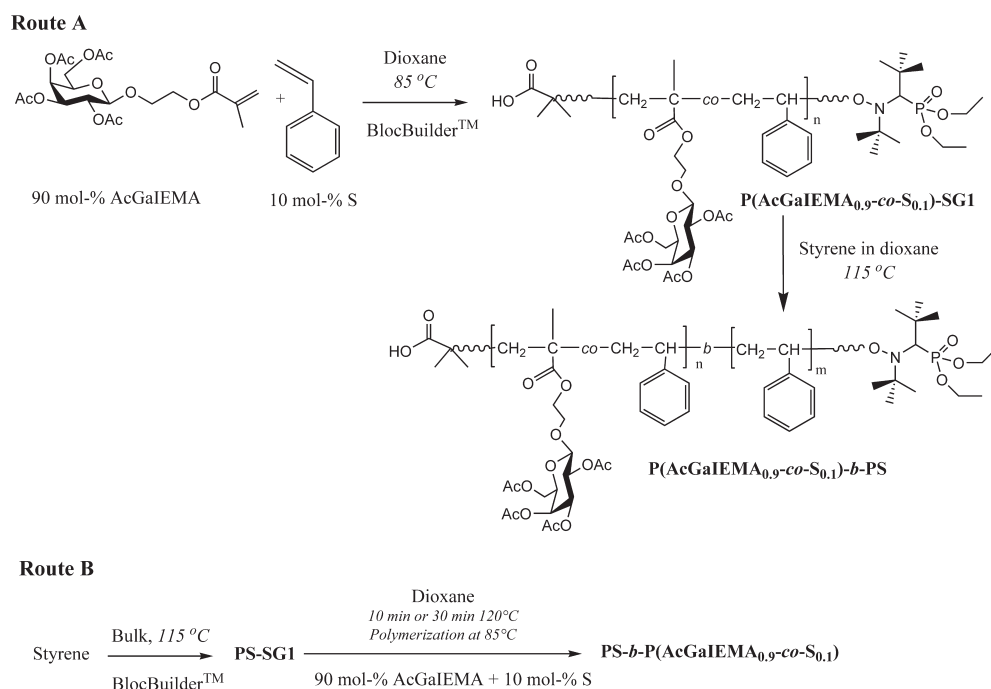
This article reports on the synthesis of a novel amphiphilic glycopolymers via NMP. The polymerization of the protected methacrylic ester glycomonomer was performed at a low temperature of 85 °C using SG1-mediated controlled free-radical polymerization with the aid of a small amount of styrene. The protecting group chemistry was required to perform the synthesis of the diblock copolymer in homogeneous organic media. The synthesis of the diblock copolymer was investigated via two routes as depicted in Scheme 2. The copolymerization of the sugar-based methacrylate with styrene formed the first block which was further used as macroinitiator for styrene polymerization (route A in Scheme 2) or the polystyrene macroinitiator was chain extended with the glycomonomer in the presence of a 10 mol % of styrene (route B in Scheme 2).

To afford an amphiphilic block copolymer, the sugar section of the diblock was deacetylated (named P(GalEMA)). The block

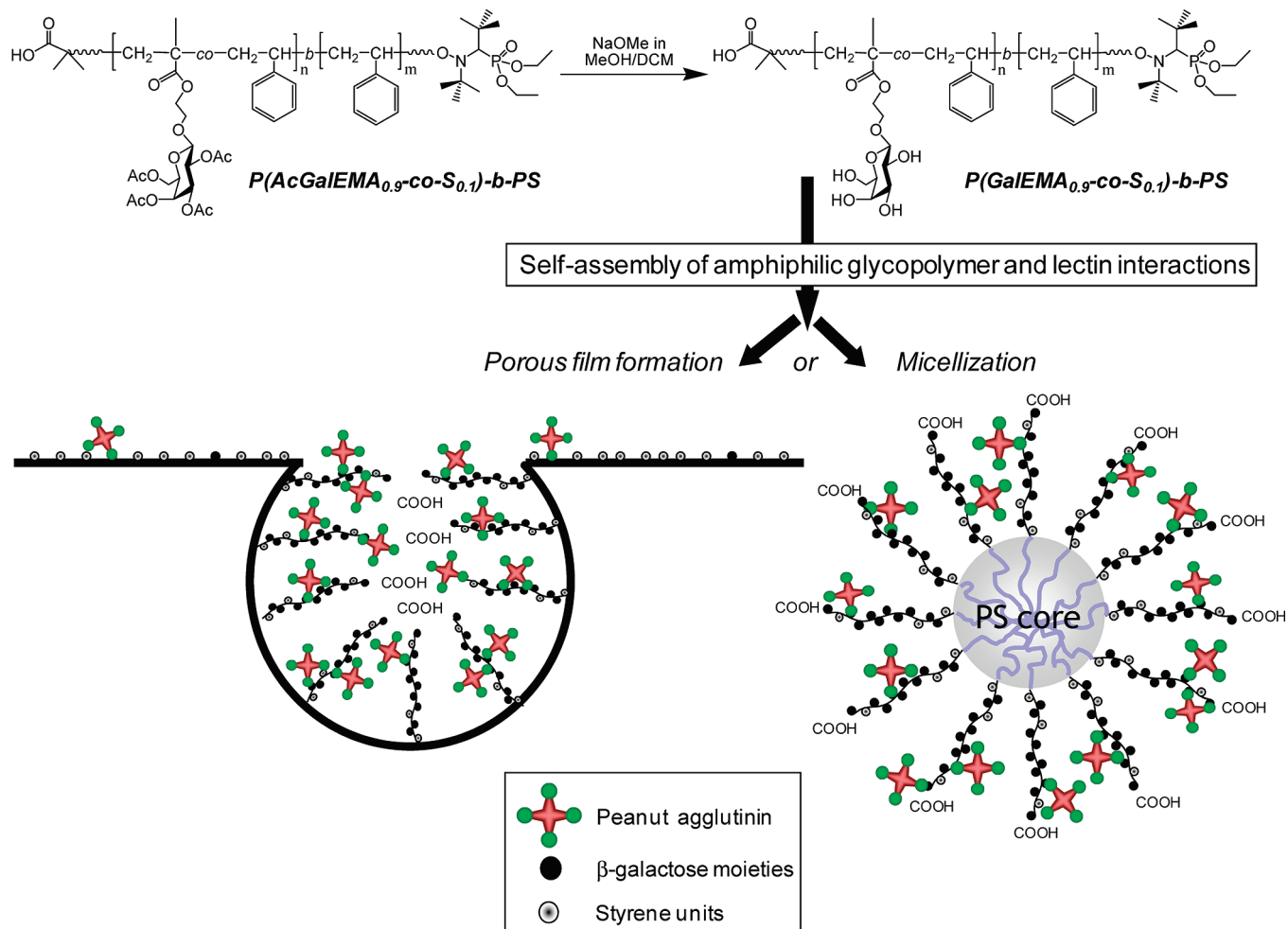
**Scheme 1. Structure of Nitroxide SG1 and SG1-Based Alkoxyamine (BlocBuilder)**



**Scheme 2. Schematic Approach to the Synthesis of Diblock Copolymers by Nitroxide-Mediated Polymerization via Either Route A To Produce Poly(2-(2',3',4',6'-tetra-*O*-acetyl- $\beta$ -D-galactosyloxy)ethyl methacrylate-*co*-styrene)-*b*-Polystyrene, named P(AcGalEMA-*co*-S)-*b*-PS, or Route B To Produce PS-*b*-P(AcGalEMA-*co*-S))**



**Scheme 3. Schematic Approach to Micelles with Glycopolymer Shell Based on  $\beta$ -Galactose Moieties and Honeycomb Structured Porous Films with Glycopolymer Enriched inside the Pore; as Materials in Solution and in Solid State That Can Selectively Recognize Peanut Agglutinin, PNA (*Arachis hypogaea*)**



copolymers were subsequently employed in the preparation of bioactive micelles with the glycopolymer block forming the shell of the self-assembled structure as depicted in Scheme 3. Furthermore, amphiphilic block copolymers can result in honeycomb structured porous films owning a nanosized substructure with glycopolymers enriched inside the pores as demonstrated in earlier studies.<sup>7,66</sup> The choice of polystyrene as hydrophobic block was driven by the previous studies showing that polymers with sufficient high glass transition temperature were required to create porous polymer films by controlled solvent evaporation.<sup>22</sup> To further screen the biofunctionality of the pendant  $\beta$ -galactose in solution and in the solid state, interactions with lectin were tested using peanut agglutinin, PNA (*Arachis hypogaea*), a  $\beta$ -galactose specific binding protein. Thanks to the carbohydrate moieties on the surfaces of the films, these films could potentially be used as cell growth templates, and the galactosylated micelles could be a candidate as a vehicle for drug delivery.

## Experimental Section

**Materials.**  $\beta$ -D-Galactose pentaacetate (98%), 2-hydroxyethyl methacrylate (HEMA, >98%), boron trifluoride diethyl etherate (purum, dist.), and anhydrous dichloromethane (>99.8%, 50–150 ppm amylene as stabilizer) were purchased from Aldrich and used without further treatment. *N,N*-Dimethylacetamide for high-performance liquid chromatography (HPLC grade) (DMAc,  $\geq 99.8\%$ ), 1,4-dioxane ( $\geq 99.0\%$ ), sodium methoxide solution (0.5 M in methanol, reagent grade),

methanol (anhydrous, 99.8%), and carbon disulfide ( $\text{CS}_2$ ,  $\geq 99.9\%$ ) from Aldrich were also used as purchased. Styrene (S, 99%) bought from Aldrich was passed through a basic alumina column before use. The *N*-(2-methylpropyl)-*N*-(1-diethylphosphono-2,2-dimethylpropyl)-*O*-(2-carboxylprop-2-yl)hydroxylamine initiator (the so-called BlocBuilder, 99%) and the *N*-tert-butyl-*N*-(1-diethylphosphono-2,2-dimethylpropyl) nitroxide (SG1, 88.4%) were kindly supplied by Arkema. Diethylphosphite (94%, Aldrich) was distilled before use as internal standard for phosphorus NMR. Lectin from *Arachis hypogaea* (PNA, Affinity purified and FITC conjugated, lyophilized powder) and Concanavalin A (ConA, Type IV and FITC labeled, lyophilized powder) from *Canavalia ensiformis* (Jack bean) were purchased from Aldrich and used without modifications. 0.01 M phosphate-buffered saline (PBS) at pH 7.4 was prepared by dissolving the powder from a sachet purchased from Sigma into 1 L of distilled water.

**Synthesis.** *Synthesis of 2-(2',3',4',6'-Tetra-O-acetyl- $\beta$ -D-galactosyloxy)ethyl Methacrylate (AcGalEMA).*  $\beta$ -D-Galactose pentaacetate (5.00 g,  $1.28 \times 10^{-2}$  mol) and 2-hydroxyethyl methacrylate, HEMA (1.27 mL,  $1.35 \times 10^{-2}$  mol), were measured into a 250 mL one-neck round-bottom flask and together with some 3 Å molecular sieves. Anhydrous dichloromethane (50 mL) was added to the stirred flask with nitrogen surroundings. The reaction started when boron trifluoride diethyl etherate (3.95 mL,  $4.54 \times 10^{-2}$  mol) was introduced over 30 min via a gastight syringe while maintaining the flow of nitrogen through the flask. After purging the solution for



**Table 1. Nitroxide-Mediated Polymerization of 2-(2',3',4',6'-Tetra-*O*-acetyl- $\beta$ -D-galactosyloxy)ethyl Methacrylate (AcGalEMA) and Styrene (S); Synthesis of First Blocks and Corresponding Diblock Copolymers**

expt	polymer	<i>T</i> (°C)	[AcGalEMA] <sub>0</sub> (mol L <sup>-1</sup> )	[S] <sub>0</sub> (mol L <sup>-1</sup> )	[I] <sub>0</sub> <sup>a</sup> (mol L <sup>-1</sup> )	[SG1] <sub>0</sub> / [I] <sub>0</sub>	time (h)	conv (%)	<i>M</i> <sub>n</sub> (SEC, calibPS) (g mol <sup>-1</sup> )	<i>M</i> <sub>w</sub> / <i>M</i> <sub>n</sub>	<i>M</i> <sub>n</sub> (SEC,DLS) (g mol <sup>-1</sup> ) (dn/dc in THF, 40 °C)
1 <sup>b</sup>	P(AcGalEMA <sub>0.9-co-S</sub> <sub>0.1</sub> )	85	2.5	0.23	$1.6 \times 10^{-2}$		2.7	45	18 300	1.26	40 600 (0.072)
2 <sup>b</sup>	P(AcGalEMA <sub>0.9-co-S</sub> <sub>0.1</sub> )- <i>b</i> -PS	115		7.5	$5.7 \times 10^{-3}$		3.8	51	48 400	1.44	85 300 (0.122)
3 <sup>c</sup>	PS <sub>41</sub> <sup>d</sup>	115		8.7	$8.7 \times 10^{-2}$		3.0	43	5 000	1.15	
4 <sup>b</sup>	PS- <i>b</i> -P(AcGalEMA <sub>0.9-co-S</sub> <sub>0.1</sub> )	120 + 85 <sup>e</sup>	1.1	0.11	$5.7 \times 10^{-3}$	0.054	2.7	48	21 700	1.34	
5 <sup>b</sup>	PS- <i>b</i> -P(AcGalEMA <sub>0.9-co-S</sub> <sub>0.1</sub> )	120 + 85 <sup>f</sup>	2.5	0.26	$1.4 \times 10^{-2}$	0.054	2.5	79	32 400	1.50	73 340 (0.085)
6 <sup>c</sup>	PS <sub>180</sub> <sup>g</sup>	115		8.7	$2.2 \times 10^{-2}$		5	50	21 800	1.28	
7 <sup>b</sup>	PS- <i>b</i> -P(AcGalEMA <sub>0.9-co-S</sub> <sub>0.1</sub> )	120 + 85 <sup>f</sup>	2.5	0.27	$1.2 \times 10^{-2}$	0.059	2.5	72	79 900	1.35	109 900 (0.104)

<sup>a</sup> [I]<sub>0</sub> corresponds to the initial concentration of initiator which is either the molecular alkoxyamine (i.e., BlocBuilder) for the first block synthesis or the first block macro(alkoxyamine) for the diblock copolymer synthesis. <sup>b</sup> Polymerization carried out in 1,4-dioxane. <sup>c</sup> Polymerization carried out in bulk. <sup>d</sup> PS<sub>41</sub>-SG1 used as macroinitiator for the synthesis of diblock copolymer of experiments 4 and 5. <sup>e</sup> Initiation period at 120 °C for 10 min. <sup>f</sup> Initiation period at 120 °C for 30 min. <sup>g</sup> PS<sub>180</sub>-SG1 used as macroinitiator for the synthesis of diblock copolymer of experiment 7.

another 20 min, the flask was sealed and left stirring at room temperature for 42 h to allow maximum conversion. The final suspension was filtered through a sintered glass funnel and washed with saturated salt solution. The bottom organic phase was removed under reduced pressure, and the resulting oily light yellow mixture was purified by column chromatography using hexane/ethyl acetate (ratio 3:2) as eluent. The light yellow oil exit the column with the *R*<sub>f</sub> value of 0.4 (3.98 g, 63%). <sup>1</sup>H NMR (CDCl<sub>3</sub>, 400 MHz)  $\delta$  (ppm): 1.98 (s, 3H, CH<sub>3</sub>), 2.00, 2.04, 2.07, 2.17 (s, 12H, CH<sub>3</sub>), 3.93 (m, 2H, O-CHH), 4.00 (m, 1H, sugar moiety CHH), 4.15 (m, 2H, CHH-O), 4.33 (m, 1H, sugar moiety CHH) (m, 1H, sugar moiety CH), 4.57 (d, 1H, sugar moiety CHH), 5.01 (dd, 1H, sugar moiety CH), 5.24 (dd, 1H, sugar moiety CH), 5.41 (s, 1H, sugar moiety CH), 5.62 (s, 1H, Me-C=CHH), 6.15 (s, 1H, Me-C=CHH).

**SG1-Mediated Copolymerization of AcGalEMA and Styrene (Experiment 1 in Table 1).** In a typical experiment, AcGalEMA (1.96 g,  $4.34 \times 10^{-3}$  mol) was first measured in a 25 mL one-neck round-bottom flask, and 10 mol % of styrene ( $4.60 \times 10^{-2}$  g,  $4.34 \times 10^{-4}$  mol) based on the amount of AcGalEMA used was carefully introduced into the same flask. Dioxane ( $2.07 \times 10^{-3}$  g,  $2.34 \times 10^{-5}$  mol) was later used to dissolve the monomers in the flask. The BlocBuilder alkoxyamine initiator ( $9.10 \times 10^{-3}$  g,  $2.39 \times 10^{-5}$  mol) was finally added to the solution. The flask was capped using a rubber septa and was thoroughly purged with nitrogen for 30 min before it was sealed. Polymerization starts when the flask was immersed into a preheated oil bath set at 85 °C. Aliquots were taken at time intervals to monitor the polymerization kinetics. The monomer conversions were determined using <sup>1</sup>H NMR by taking crude mixtures from the aliquots and dissolving them into CDCl<sub>3</sub>. AcGalEMA monomer conversions of the polymers were calculated by comparing the anomeric proton of AcGalEMA monomer at 5.6 ppm to two protons at 5.3–5.5 ppm each from the AcGalEMA monomer and P(AcGalEMA<sub>0.9-co-S</sub><sub>0.1</sub>) polymer. The final copolymer from the crude solution was precipitated gradually in 10-fold excess of diethyl ether (three times), filtered, and dried under reduced pressure at room temperature for at least one night before using it for chain extension experiments. The purified copolymers were obtained as a fine and colorless powder. The molar composition of styrene and sugar-based monomer in the copolymer was determined by comparing the integrals of a proton of P(AcGalEMA) six-membered cyclic ring at 5.33 ppm and the aromatic protons of polystyrene at 7.00 ppm. The <sup>1</sup>H NMR spectrum was obtained by dissolving 10 mg of purified copolymer in CDCl<sub>3</sub>.

**Chain Extension Solution Polymerization of P(AcGalEMA<sub>0.9-co-S</sub><sub>0.1</sub>) with Styrene in Dioxane (Experiment 2 in Table 1).** Purified P(AcGalEMA<sub>0.9-co-S</sub><sub>0.1</sub>) from experiment 1 (0.30 g,  $5.33 \times 10^{-6}$  mol, *M*<sub>n</sub>(SEC,LS) = 56 250 g mol<sup>-1</sup>, *M*<sub>w</sub>/*M*<sub>n</sub> = 1.42),

was measured into a 25 mL single-neck round-bottom flask followed by careful addition of styrene (0.728 g,  $6.99 \times 10^{-3}$  mol). The mixture was dissolved in dioxane (0.17 g,  $1.54 \times 10^{-3}$  mol) and thoroughly bubbled with nitrogen for 40 min before being sealed and lowered into a preheated oil bath of 115 °C. Samples were withdrawn at different time intervals. Conversions were obtained by comparing the aromatic protons of styrene and its polymer at the region between 6.5 and 7.5 ppm with the vinylic proton of styrene at 6.1 ppm. The diblock copolymer was precipitated three times in diethyl ether to yield a fine white powder.

**Synthesis of Polystyrene Macroinitiator Using the BlocBuilder Alkoxyamine Initiator (Experiment 3 in Table 1).** The reaction was carried out in bulk where styrene (8.0 g,  $7.68 \times 10^{-2}$  mol) was measured into a 25 mL single-neck round-bottom flask followed by the dissolution of BlocBuilder (0.29 g,  $7.68 \times 10^{-4}$  mol) in styrene. The flask was thoroughly purged with nitrogen for 30 min and sealed. Polymerization was carried out at 115 °C, and aliquots were taken at time intervals for the duration of 3 h to monitor its kinetics. Aliquots at different time intervals were diluted directly in CDCl<sub>3</sub> for <sup>1</sup>H NMR measurements. Conversions were obtained by comparing the aromatic protons of styrene and its polymer at the region between 6.5 and 7.5 ppm with the vinylic proton of styrene at 6.1 ppm. The final PS-SG1 macroinitiator was precipitated with ethanol/water mixture (ratio 5:1) three times, filtered, and dried under reduced pressure overnight at room temperature, yielding a colorless fine powder.

**SG1-Mediated Chain Extension Copolymerization of PS Macroinitiator with AcGalEMA and Styrene (Experiments 4, 5, and 7 in Table 1).** In experiment 7, AcGalEMA (0.97 g,  $2.11 \times 10^{-3}$  mol) and 10 mol % styrene (0.022 g,  $2.11 \times 10^{-4}$  mol) based on the amount of AcGalEMA used were measured into a 25 mL single-necked round-bottom flask. This is followed by another 5 mol % of free SG1 (1.80 × 10<sup>-4</sup> g,  $6.11 \times 10^{-7}$  mol) based on the amount of PS<sub>180</sub> macroinitiator used. Free SG1 was prepared by first dissolving 1.80 × 10<sup>-2</sup> g of free SG1 in 10 mL of dioxane and transferring 0.1 mL using a microsyringe into the reaction mixture. PS<sub>180</sub> macroinitiator (0.22 g,  $1.17 \times 10^{-5}$  mol) was then added to the mixture, and dioxane (0.88 g,  $1.0 \times 10^{-2}$  mol) was used to dissolve the mixture. The flask was thoroughly degassed for 30 min before it was sealed and placed into a preheated oil bath at 120 °C for 30 min. The round-bottom flask was swiftly transferred into another oil bath prepared at 85 °C and left to polymerize. AcGalEMA monomer conversions of the polymers were calculated by comparing the anomeric proton of AcGalEMA monomer at 5.6 ppm to two protons at 5.3–5.5 ppm each from the AcGalEMA monomer and P(AcGalEMA<sub>0.9-co-S</sub><sub>0.1</sub>) polymer. The crude reaction mixture was precipitated in diethyl ether for three times, and the filter product was dried under reduced pressure overnight to yield a white solid powder.

**Deacetylation of Galactose Polymers.** 1 M solution of sodium methoxide was first prepared by concentrating the commercially available 0.5 M sodium methoxide in methanol under reduced pressure. 0.07 g of P(AcGalEMA<sub>0.9-co-S</sub><sub>0.1</sub>)-*b*-PS copolymer from experiment 7 (Table 1) was dissolved in 2 mL of CHCl<sub>3</sub>/CH<sub>3</sub>OH mixture (ratio 1:1) in a 10 mL round-bottom flask. The solution was degassed with N<sub>2</sub> for 15 min before 0.21 mL of the prepared 1 M sodium methoxide was added to the solution. After 5 s, a white precipitate was observed, and the mixture was stirred under N<sub>2</sub> atmosphere for another 40 min to allow maximum deacetylation of the copolymers. The mixture was dried overnight under reduced pressure to give a colorless solid. The product was dissolved in DMAc and dialyzed (membrane cutoff of 3500 g mol<sup>-1</sup>) against water overnight to remove Na<sup>+</sup> ions. The amphiphilic diblock copolymer was named PS-*b*-P(GalEMA<sub>0.9-co-S</sub><sub>0.1</sub>) (deacetylation of experiment 7 copolymer).

**Micellization of PS-*b*-P(GalEMA<sub>0.9-co-S</sub><sub>0.1</sub>) Amphiphilic Copolymer.** Micelles were prepared by first dissolving 50 mg of the deacetylated diblock copolymer (from diblock copolymer of experiment 7 in Table 1) into 2 mL of DMAc, and 3 mL of distilled water was gradually added dropwise into the polymer mixture with stirring. The resulted mixture was dialyzed (membrane cutoff of 3500 g mol<sup>-1</sup>) against distilled water overnight to remove DMAc.

**Arachis hypogaea Turbidimetry Binding Assay.** 2 mg mL<sup>-1</sup> of peanut agglutinin was first prepared in 0.01 M phosphate-buffered saline (PBS) at pH 7.4. 500  $\mu$ L of this lectin solution was transferred into a masked semi-microcell and placed into the holding block of the spectrometer for temperature equilibration at 25  $^{\circ}$ C, and a baseline was subsequently taken. A solution of 50  $\mu$ L containing the galactose ligand diblock copolymer in PBS solution (500  $\mu$ M per galactose residue) was added into the cuvette containing the lectin solution. The solution in the cuvette was gently mixed using a pipet and immediately returned into the holding block where an absorbance at 420 nm was recorded for 10 min. A control using the exact same conditions was performed by replacing PNA lectin with ConA lectin.

**Dynamic Light Scattering Measurements of Glycoparticles with Arachis hypogaea Conjugation.** Micelles were first obtained by dialysis as described in the above section and were further diluted to 0.1 mg mL<sup>-1</sup>. An initial measurement of this polymeric ligand solution (500  $\mu$ L) at 25  $^{\circ}$ C was conducted using the dynamic light scattering analyzer. 200  $\mu$ L of peanut agglutinin in PBS at pH 7.4 (1 mg mL<sup>-1</sup>) was pipetted into the low volume disposable cuvette of polymeric ligand solution with gentle mixing using a pipet to start the binding assay. The mixed solution containing the polymeric ligands and peanut agglutinin was immediately placed onto the holding block of the analyzer for measurements for a duration of 33 min.

**Fabrication of Honeycomb Structured Porous Films.** The PS-*b*-P(GalEMA<sub>0.9-co-S</sub><sub>0.1</sub>) deacetylated diblock copolymer (from diblock copolymer of experiment 7 in Table 1) was used either alone for film formation or in a mixture with a 6 arm star PS,  $M_n = 36\,000$  g mol<sup>-1</sup>, PDI = 1.14. The 6-arm star PS was synthesized using a previously published procedure.<sup>67</sup> PS-*b*-P(GalEMA<sub>0.9-co-S</sub><sub>0.1</sub>) was dissolved in carbon disulfide to prepare a 3 g L<sup>-1</sup> solution. For a mixture of polymers, PS-*b*-P(GalEMA<sub>0.9-co-S</sub><sub>0.1</sub>) and 6-arm star PS (1:1 w/w) were dissolved in carbon disulfide to a concentration of 3 g L<sup>-1</sup>. An aliquot of 40  $\mu$ L for each polymer solution was cast onto a glass coverslip (10 mm diameter) inside a custom-made casting box. Relative humidity and temperature were controlled at 67% and 23  $^{\circ}$ C, respectively. No direct airflow was applied for the casting of the polymer films.

**Immobilization of Fluorescent PNA Protein on Porous Films.** Fluorescent PNA protein is utilized to determine the location of glycopolymers on the porous film when it was cast. 0.5 mg of fluorescent PNA was dissolved in 1 mL of pH 7.4 PBS (phosphate buffered saline) buffer solution. The solution was

introduced dropwise onto the porous films cast from a polymer mixture of PS-*b*-P(GalEMA<sub>0.9-co-S</sub><sub>0.1</sub>) (deacetylated diblock copolymer from diblock copolymer of experiment 7 in Table 1) and 6-arm star PS. The lectin solution was left to penetrate into the pores of the porous films over 3 days in the dark to avoid the diminishment of fluorescent PNA. Unattached fluorescent PNA was removed by first washing the film several times with pH 7.4 PBS buffer solution and subsequently immersing it into pH 7.4 PBS buffer solution and distilled water for washing over another 3 days. The exact same immobilization conditions were performed by replacing the FITC PNA lectin with FITC ConA lectin using a porous film cast from a polymer mixture of PS-*b*-P(GalEMA<sub>0.9-co-S</sub><sub>0.1</sub>) and 6-arm star PS. In addition, porous film cast from unfunctionalized 6-arm star PS was also loaded with FITC PNA lectin as a control.

**Analysis.** *Nuclear Magnetic Resonance (NMR) Spectroscopy.* All NMR spectra were recorded using a Bruker 400 MHz spectrometer at 25  $^{\circ}$ C. <sup>1</sup>H and <sup>13</sup>C measurements were made at frequencies of 400.13 and 100.6 MHz, respectively, and calibrated with respect to the solvent signal. <sup>31</sup>P spectra were obtained in 5 mm sample tubes at 161.97 MHz, and chemical shifts were measured from 85% phosphoric acid (0 ppm) for <sup>31</sup>P NMR spectra. Quantitative analysis was performed using diethylphosphite as internal standard (see Supporting Information). AcGalEMA monomer, P(AcGalEMA<sub>0.9-co-S</sub><sub>0.1</sub>) polymer, PS macroinitiator, and all the diblock copolymers were analyzed using deuterated chloroform as solvent. Deuterated dimethyl sulfoxide was used for the deacetylated polymers.

**Size Exclusion Chromatography (SEC).** Characterizations of the copolymers were performed at 30  $^{\circ}$ C with THF as eluent at a flow rate of 1 mL/min and an injection volume of 100  $\mu$ L. The SEC device was equipped with three Waters Styragel columns HR 0.5, 2, and 4 working in series (separation range  $1 \times 10^2$ – $3 \times 10^6$  g mol<sup>-1</sup>), a refractive index detector ERC 7515-A (a white light and the wavelength from the tungsten filament), and a Wyatt Dawn DSP MALLS (multiangle light scattering) detector (wavelength of 632.8 nm and a power of 5 mW). The number-average molar mass ( $M_n$ ) and the polydispersity index ( $M_w/M_n$  = PDI) were calculated from a polystyrene calibration. For the glycopolymer, absolute molar masses were determined using the MALLS detector, and the average  $dn/dc$  of the copolymer was measured online with the RI detector. All the experimental values are reported in Table 1. All the polymers samples were prepared at 1–5 g L<sup>-1</sup> concentration and filtered through PVDF 0.45  $\mu$ m filters.

**Fourier Transform Infrared Red Spectroscopy (FT-IR).** A Bruker IFS\S Fourier transform spectrometer equipped with a tungsten halogen lamp, a KBr beam splitter with a mid-Infrared red source, and a DTGS detector were used for the attenuated total reflectance (ATR) measurements. The spectra were recorded in the spectral region of 400–4000 cm<sup>-1</sup> and were obtained from 64 scans with a resolution of 4 cm<sup>-1</sup>. A background measurement was taken before a white solid powder of the polymers was loaded onto the ATR unit for measurements.

**UV-vis Spectrophotometer.** A UV-vis spectrophotometer (Cary 300) equipped with a temperature controller was used for the turbidity assay of the ligand/protein conjugation. Absorbance data were recorded at 420 nm for 10 min at 1.2 Hz.

**Dynamic Light Scattering (DLS).** Particles sizes were determined using a Malvern Zetasizer nano ZS with a laser of 4 mW (He-Ne),  $\lambda = 632$  nm, 173 $^{\circ}$ , backscatter. The micellar solutions were measured straight after dialysis and with different dilutions using distilled water at automatic run times. Lectin binding experiments were measured with the average of five runs at 10 s for each run. The mean diameter was obtained from the arithmetic mean using the number distributed diameter of each particle size.

**Transmission Electron Microscopy (TEM).** The TEM micrographs were obtained using a JEOL 1400 transmission electron microscope at an accelerating voltage of 100 kV. The sample were prepared by casting an aqueous solution of deacetylated

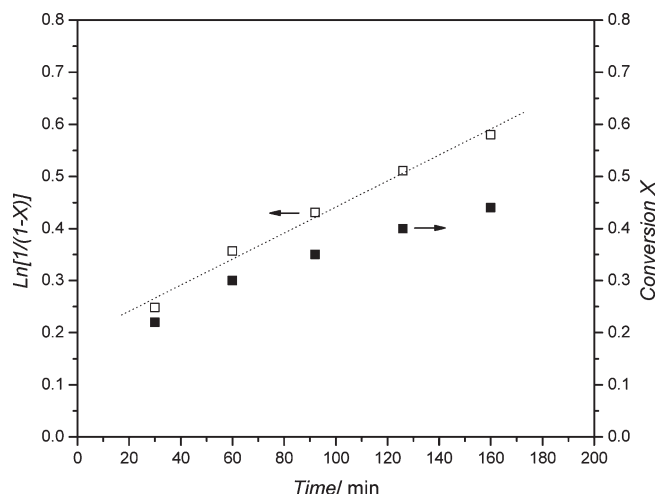


**Figure 1.** Pseudo-first-order kinetic and conversion plots of SG1-mediated copolymerization of AcGalEMA in presence of 9 mol % of styrene vs AcGalEMA monomer. Reaction conducted in 1,4-dioxane at 85 °C; the experimental conditions of experiment 1 are gathered in Table 1.

PS-*b*-P(GalEMA<sub>0.9-co</sub>-S<sub>0.1</sub>) diblock copolymer (from experiment 7) micellar solution (1 g L<sup>-1</sup>) onto a copper grid coated with Formvar. Positive staining using osmium tetroxide (OsO<sub>4</sub>) vapor was carried out by keeping the deposited micelles on the copper grid in an enclosed glass Petri dish with OsO<sub>4</sub> vapor overnight. Negative staining was performed by casting a tiny drop of (2% w/w) of phosphotungstic acid (PTA) onto the already deposited micelles and left standing for 45 s. Excess acid was drained using a filter paper. The images taken were also used to obtain an average particle size using the equation  $D_n = \sum n_i D_i / \sum n_i$ . Twenty particles were each measured from the images and calculated using the equation, where  $D_n$  is the number-average diameter.<sup>68</sup>

**Scanning Electron Microscopy (SEM).** Scanning electron microscopy (SEM) of the films was performed on a Hitachi S-900 and a Hitachi S-4500 FESEM. The glass supported and self-standing films were fixed to copper stubs with carbon adhesive tape. Prior to the analysis the specimens were sputter-coated with 10 nm of chromium (EMITECH K575× high resolution).

**Confocal Microscopy.** The presence of fluorescing PNA protein on the porous film was analyzed and determined using a Leica TCS SP confocal DMIRB inverted microscope with three channel (488, 568, and 647 nm) excitation and a Leica HCS 40× objective. Because of the porosity of films, between the inverted sample and the glass coverslip, distilled water was introduced to aid analysis.

## Results and Discussion

The glycopolymer based on galactose used in this work plays an important role in many biological processes such as the selective targeting of hepatocytes using the unique interaction between the asialoglycoprotein receptor (ASGPR) and galactose.<sup>69</sup> In order to obtain synthetic polymer with bioactive carbohydrates, a galactosylated monomer synthesized by the glycosylation of 2-hydroxyethyl methacrylate at the first position of  $\beta$ -D-galactose pentaacetate was carried out.  $\beta$ -Stereoselectively in the glycosylation reaction resulted in the attachment of HEMA in the first position of the galactose sugar ring. This reaction had proven to be selective and efficient.<sup>70,71</sup> In the subsequent step, the monomer was polymerized using NMP. SG1-mediated polymerization has been reported to be successful in the polymerization of methacrylate-based monomers using a low proportion of styrene. This system was found to lead to well-defined polymers based on methacrylic acid and styrene.<sup>65</sup>

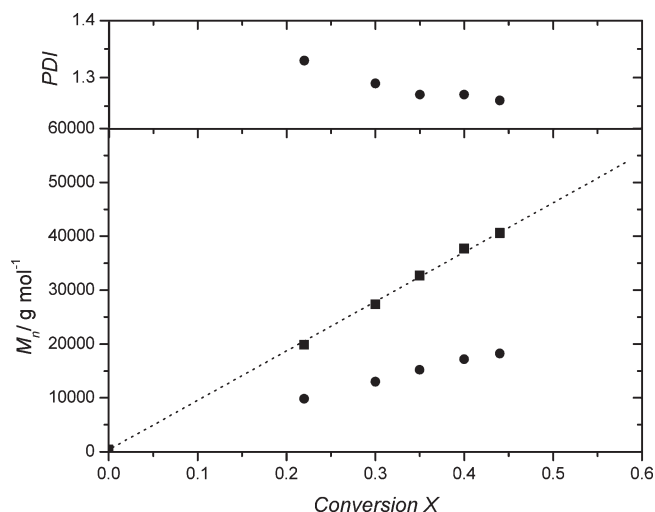


**Figure 2.** Evolution of number-average molar mass and polydispersity index, PDI, for P(AcGalEMA<sub>0.9-co</sub>-S<sub>0.1</sub>) vs monomer conversion ( $X$ ). Dotted line is the theoretical  $M_n$ , (■) represents the  $M_n$  measured by SEC with light scattering detector, and (●) shows the  $M_n$  of P(AcGalEMA<sub>0.9-co</sub>-S<sub>0.1</sub>) calculated on the basis of a polystyrene calibration. The experimental conditions of experiment 1 are reported in Table 1.

**Route A: Synthesis of Poly(2-(2',3',4',6'-tetra-*O*-acetyl- $\beta$ -D-galactosyloxy)ethyl methacrylate-*co*-styrene)-*b*-Polystyrene, P(AcGalEMA<sub>0.9-co</sub>-S<sub>0.1</sub>)-*b*-PS via NMP.** In this experiment, polymerizing a methacrylate-based galactose monomer using SG1-mediated polymerization was investigated for the synthesis of the first block. The use of 10 mol % of styrene with respect to AcGalEMA monomer was employed. The selection of solvent was effortless as dioxane being a solvent generally used for nitroxide-mediated polymerization easily dissolves the AcGalEMA monomer, styrene, and the random copolymer. The polymerization proceeds in a controlled fashion with high radical concentration generated at the start of the reaction but was followed by a constant radical flux throughout the polymerization duration (Figure 1).

The dependence of molecular weight on conversion is in agreement with a controlled process as the growing chains were constant through the course of reaction (Figure 2). SEC chromatograms obtained from using a light scattering detector reveal near-symmetrical curves at different conversions (Figure 3), which was indicative of a well-controlled polymerization with a minimum amount of dead chains at the lower molecular end of the SEC traces. The number-average molar mass increases linearly with conversion, and the polydispersity indexes of the polymers reduce to 1.26 at 45% conversion. Number-average molar masses determined using the SEC calibrated with polystyrene standards deviate from the theoretical values as depicted in Figure 2. The deviation could be assigned to the vast difference in hydrodynamic volume of the P(AcGalEMA<sub>0.9-co</sub>-S<sub>0.1</sub>) polymers in THF when compared to polystyrene. To be able to find a conclusive value for our experimental molar masses, the light scattering detector coupled online with SEC was employed. For that purpose, the average  $dn/dc$  of each copolymer was experimentally measured with the refractometer detector, and the values are reported in Table 1. The absolute molar masses of the sugar-based copolymers were systematically higher than the molar masses obtained using polystyrene calibration.

The ability to reinitiate the SG1-capped P(AcGalEMA<sub>0.9-co</sub>-S<sub>0.1</sub>) methacrylate-based polymer determines whether a



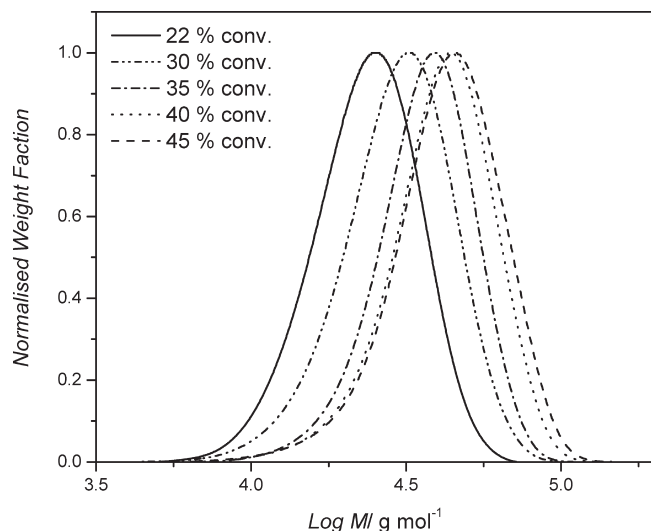


**Figure 3.** Size exclusion chromatograms of P(AcGalEMA<sub>0.9</sub>-co-S<sub>0.1</sub>) obtained at different monomer conversion during the copolymerization in 1,4-dioxane at 85 °C. The experimental conditions of experiment 1 are reported in Table 1.

pure amphiphilic diblock copolymer can be obtained.<sup>63</sup> Preliminary studies of the reinitiation of P(AcGalEMA<sub>0.9</sub>-co-S<sub>0.1</sub>) macroinitiator revealed some lower molecular weight tailing when using dioxane as solvent (Figure 4). To further understand this observation, the P(AcGalEMA<sub>0.9</sub>-co-S<sub>0.1</sub>) macroinitiator was analyzed using <sup>31</sup>P NMR quantitative analysis. The NMR spectrum showed signals at 23 and 26 ppm (see Figure SI-4 in Supporting Information), which indicates the presence of end-functionalized phosphorus SG1-nitroxide in the copolymer. From the peak integration, the percentage of chains terminated by the alkoxyamine group was 81%. This result indicates about 19% of the alkoxyamine groups were lost leading to low molecular weight tailing (Figure 4).

**Route B: Synthesis of Polystyrene-*b*-Poly(2-(2',3',4',6'-tetra-*O*-acetyl- $\beta$ -D-galactosyloxy)ethyl methacrylate-co-styrene), PS-*b*-P(AcGalEMA<sub>0.9</sub>-co-S<sub>0.1</sub>) via NMP.** Diblock copolymers were first generated with an initial polystyrene block and subsequently extended via NMP with 90 mol % of AcGalEMA monomer and 10 mol % of styrene for the synthesis of the second block (see route B depicted in Scheme 2). Preparing the polystyrene block first removes the risk of the decomposition of the glycopolymers since the sugar units are not exposed for a long time to the high reaction temperatures of the styrene polymerization (115 °C). Moreover, the reinitiating efficiencies of both SG1-end-capped macroinitiator made either by the copolymerization of AcGalEMA and styrene (route A in Scheme 2, Figure 4) or by styrene polymerization (route B in Scheme 2) can be compared. The first-order kinetic plot of styrene polymerization shows a linear plot (see Figure SI-1 in Supporting Information) which is in agreement with a constant radical concentration throughout the polymerization. Reaction proceeds in a controlled fashion as witness from the linear molecular weight vs conversion plot (Figure 5). Polydispersity of polystyrene decreases distinctively with increasing conversion, as the main equilibrium in nitroxide-mediated polymerization is established. A narrow polydispersity of 1.15 was obtained at a final conversion of 43% (Figure 5). The SEC chromatograms of PS samples clearly shifted toward high molar mass with increasing conversion (see Figure SI-2 in Supporting Information). The conversion of the first block was kept below 50% for both route A and B to minimize irreversible termina-

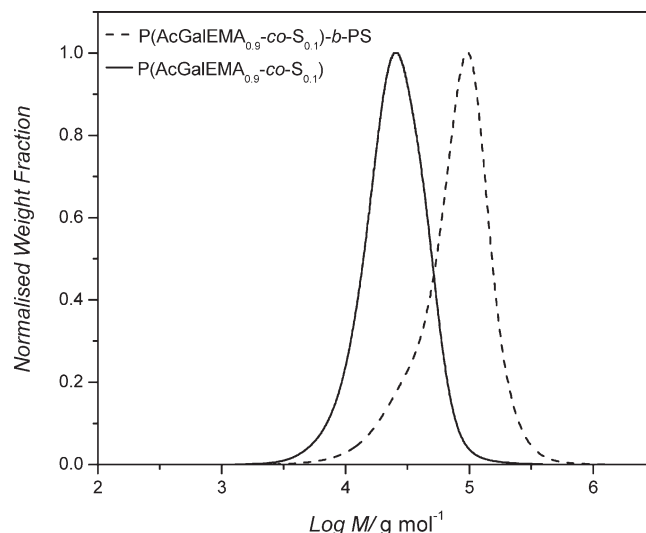


**Figure 4.** Size exclusion chromatograms of chain extension polymerization of P(AcGalEMA<sub>0.9</sub>-co-S<sub>0.1</sub>) macroinitiator with styrene in 1,4-dioxane at 115 °C yielding P(AcGalEMA<sub>0.9</sub>-co-S<sub>0.1</sub>)-*b*-PS diblock copolymer. See experiments 1 and 2 in Table 1 for experimental conditions and results.

tion reactions and to favor a high fraction of living chains for both PS and P(AcGalEMA<sub>0.9</sub>-co-S<sub>0.1</sub>) macroinitiators.<sup>63</sup>

The PS-*b*-P(AcGalEMA<sub>0.9</sub>-co-S<sub>0.1</sub>) diblock copolymer was prepared using the PS<sub>41</sub>-SG1 macroinitiator dissolved in dioxane. To further rule out any chain transfer to solvent during the chain extension of AcGalEMA, a preliminary chain extension polymerization of styrene at 120 °C either in solution with dioxane or in bulk was conducted. Both experiments displayed a complete shift of the SEC curves, and no evidence of chain transfer reaction to solvent could be observed at 50% conversion of styrene monomer (see the good overlay of SEC chromatograms in Figure SI-3, Supporting Information). Moreover, the PDIs of the extended polystyrene conducted in bulk and solution using dioxane as solvent both gave values of 1.24.

For the synthesis of the PS-*b*-P(AcGalEMA<sub>0.9</sub>-co-S<sub>0.1</sub>) diblock copolymer, an additional step had to be incorporated to balance between the high activation–deactivation constant of methacrylate-based monomer<sup>62</sup> and the lower activation rate of polystyryl SG1-based macroalkoxyamine.<sup>72</sup> This can be addressed by the increase of the reaction temperature leading to the formation of block copolymers starting with polystyrene. However, high temperatures of 120 °C could not be used to polymerize AcGalEMA as the sugar monomers are generally not stable at temperatures above 120 °C;<sup>34</sup> in addition, the polymerization of methacrylate-based monomer at high temperature could result in uncontrolled reactions.<sup>65</sup> To increase the reinitiation efficiency of the PS–SG1 macroinitiator, we have designed a preinitiation step by polymerizing both AcGalEMA and styrene monomers at 120 °C in the presence of PS–SG1 macroinitiator for 10 or 30 min to encourage the polystyryl-based macroalkoxyamine homolytic cleavage for the chain extension polymerization.<sup>73</sup> After the preinitiation step, the reaction flask was immediately changed to the oil bath thermostated at 85 °C for the copolymerization experiment. However, this step must be fine-tuned in order to fully reinitiate the polystyrene block while not overburden the polymerization of AcGalEMA monomer. Additional 5 mol % of free SG1 with respect to the macroinitiator concentration was also added in the reaction medium to ensure the control of the polymerization. Figure 6 portrays

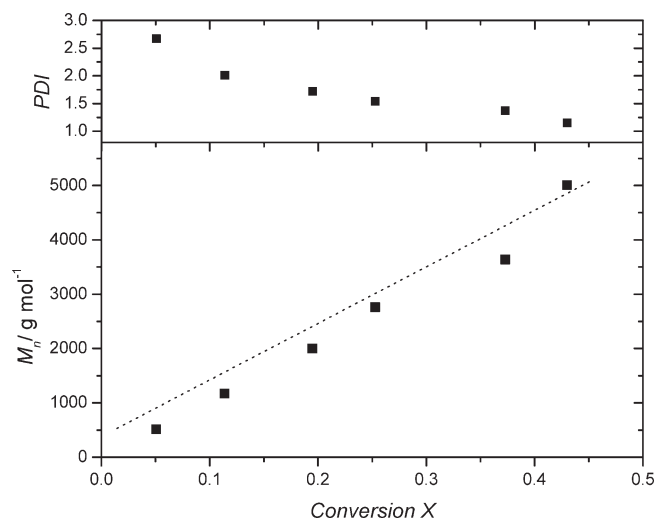


**Figure 5.** Evolution of number-average molar mass and polydispersity index, PDI, for PS macroinitiator vs styrene conversion ( $X$ ). Dotted line corresponds to the theoretical  $M_n$ . See experiment 3 in Table 1 for experimental conditions.

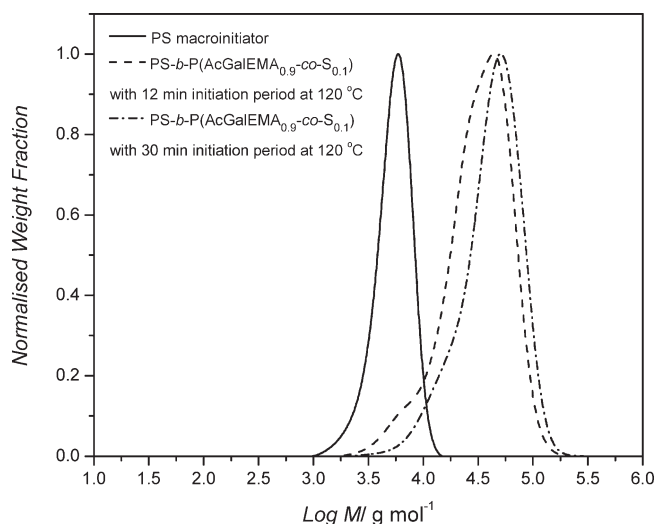


**Figure 6.** Size exclusion chromatograms of the chain extension copolymerization of PS<sub>41</sub>-macroinitiator with AcGalEMA and 10 mol % of styrene. The copolymerization was performed in 1,4-dioxane at 85 °C with an initiation period at 120 °C. See experiments 4 and 5 in Table 1 for experimental conditions.

the SEC curves of the chain extension copolymerization of AcGalEMA and styrene. Results revealed that at longer reinitiation time gave a higher PS-SG1 initiation efficiency as the recovered diblock copolymer exhibited a smaller shoulder on the low molar mass side.

**Deacetylation of PS-*b*-P(AcGalEMA<sub>0.9</sub>-co-S<sub>0.1</sub>) to PS-*b*-P(GalEMA<sub>0.9</sub>-co-S<sub>0.1</sub>).** Deacetylation reaction of the protected acetyl groups on galactose were removed with sodium methoxide as described in the Experimental Section.<sup>70</sup> In order to confirm the deacetylation process, FT-IR measurements were carried out on the polymers before and after deacetylation. The hydroxyl band above 3000 cm<sup>-1</sup> appeared after deacetylation while the carbonyl band at 1740 cm<sup>-1</sup> decreased in intensity (Figure 7). <sup>1</sup>H NMR further confirmed the successful deprotection and also confirmed the presence of pendant carbohydrate moieties on the polymer after NaOMe treatment. Integrations of the proton from the anomeric carbon of the sugar molecule and the two protons of the aliphatic carbons from the deacetylated polymer

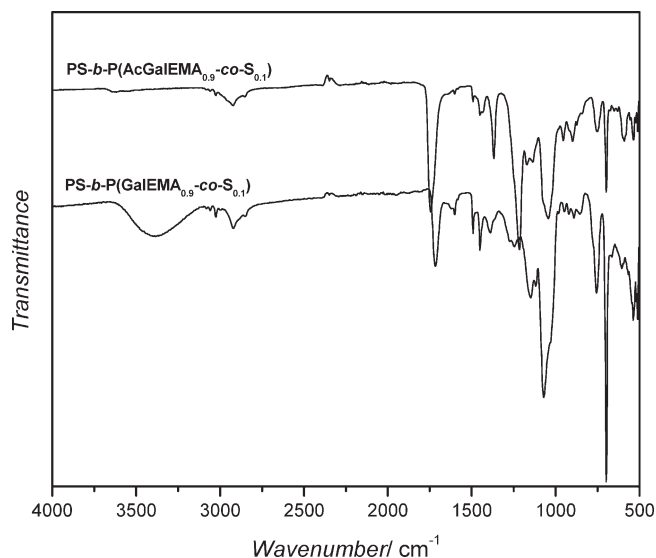


**Figure 7.** FT-IR spectrum of PS-*b*-P(AcGalEMA<sub>0.9</sub>-co-S<sub>0.1</sub>) diblock copolymer with acetylated galactose moieties (experiment 7 in Table 1) and the corresponding PS-*b*-P(GalEMA<sub>0.9</sub>-co-S<sub>0.1</sub>) deacetylated galactose moieties.

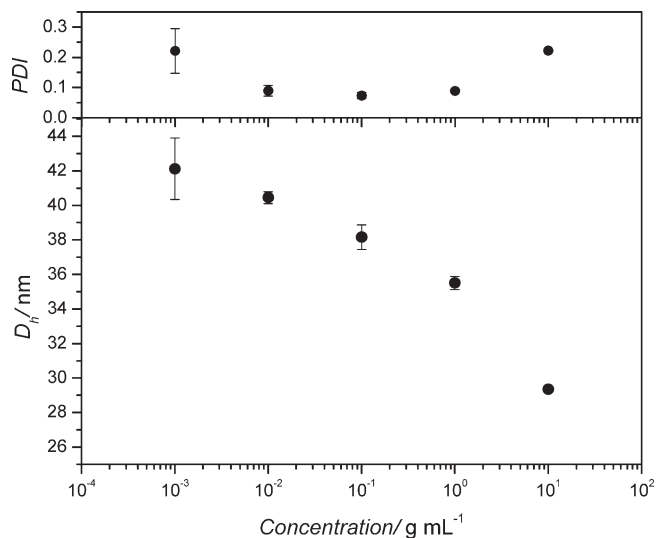


**Figure 8.** Dynamic Light scattering measurements of PS-*b*-P(GalEMA<sub>0.9</sub>-co-S<sub>0.1</sub>) micelles particles sizes and polydispersity indices vs the concentrations of micellar solutions.

backbone concluded that more than 95% of the sugar moieties were still present (see Figure SI-5 in Supporting Information).

**Particles Sizes and Morphology of PS-*b*-P(GalEMA<sub>0.9</sub>-co-S<sub>0.1</sub>) Micelles in Aqueous Medium.** The self-assembly of the amphiphilic glycopolymer synthesized from the deacetylation of the PS-*b*-P(AcGalEMA<sub>0.9</sub>-co-S<sub>0.1</sub>) diblock copolymer (experiment 7 in Table 1) was conducted in aqueous medium. It needs to be considered that the hydrophilic block contains a few units of hydrophobic styrene units; however, the formation of micelles was successful, and the styrene units did not affect the micelles formation. The high  $T_g$  (~100 °C) of polystyrene suggests that the micelles obtained could be frozen in the core.<sup>74</sup> Light scattering measurements were conducted at different concentration of micelles in solution. As shown in Figure 8, the hydrodynamic diameter decreases gradually as the concentration of the micellar solution increased. This is in contrast to most observations, where the micelle size increases with concentration. This may



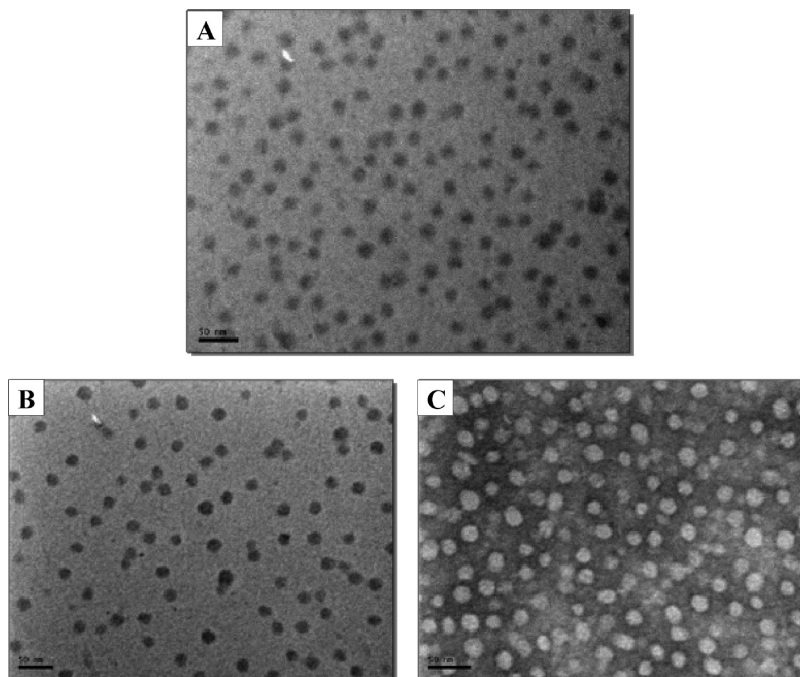


**Figure 9.** TEM images of PS-*b*-P(GalEMA<sub>0.9</sub>-*co*-S<sub>0.1</sub>) micelles unstained (A), positively stained (B), and negatively stained (C). Scale bars are 50 nm for all three images.

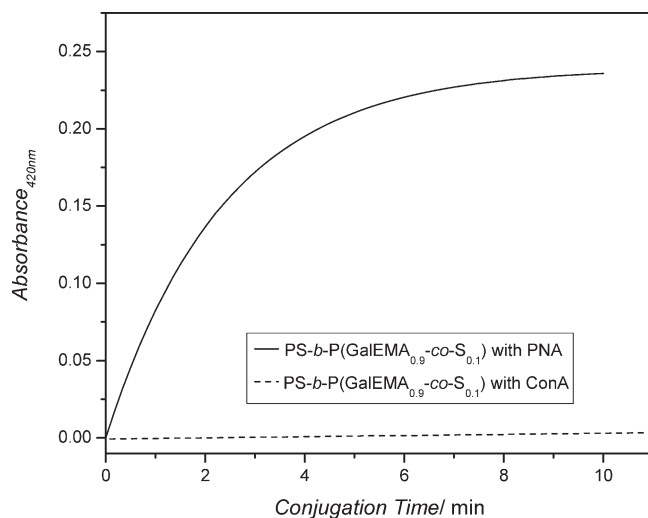


**Figure 10.** Turbidimetry assay experiment of PS-*b*-P(GalEMA<sub>0.9</sub>-*co*-S<sub>0.1</sub>) glycomicelles with peanut agglutinin and Concanavalin A.

be assigned to a decline in aggregation number or to a compression of the shell, but this is currently only subject to speculations.

TEM images of the micelles were analyzed with and without staining. Results reveal consistency between both the DLS measurements and the TEM images, taking into account that the micelles were in dry state during TEM analysis. The hydrodynamic diameter of the micelles (1 g L<sup>-1</sup> micellar solution) obtained using DLS gave sizes of 35 nm, and a smaller size of ~24 and ~25 nm was observed in the image taken from the positively stained particles and unstained particles, respectively, in the TEM. This reduction in size observed in the TEM images could be assigned to the collapsed poly(2-( $\beta$ -D-galactosyloxy)ethyl methacrylate-*co*-styrene) shell surrounding the polystyrene core.<sup>75</sup> The PTA negatively stained particles (~28 nm) appeared larger in size when compared to the unstained (~25 nm) and positively

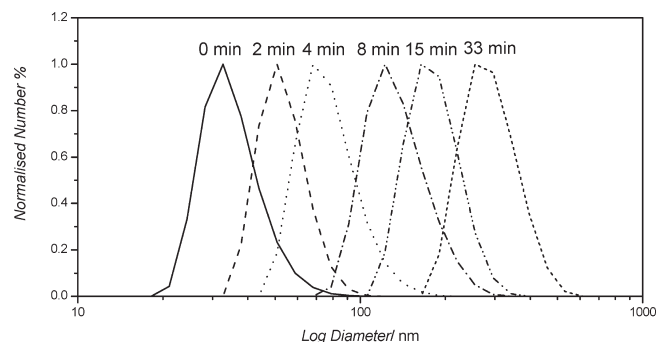


**Figure 11.** Evolution of dynamics light scattering curves of peanut agglutinin binding with PS-*b*-P(GalEMA<sub>0.9</sub>-*co*-S<sub>0.1</sub>) glycomicelles for 33 min.

stained (~24 nm) ones. This was due to the core-shell nature of the particles as the unstained and positively stained particles shows only the dense polystyrene core while the PTA negatively stained particles allows a better size average as only the surrounding of the particles are stained and not the particles core and the sparsely packed sugar shell.<sup>76</sup> TEM images at lower magnification confirm the uniformity of the micelle size (see Figure SI-6 in Supporting Information).

**Lectin Binding Assay.** To be able to prove that the bio-functionality of the galactose moieties is still active and not lost during the polymerization process and to understand how the polymeric ligands would react in the biological system, the ligand-lectin binding ability of the glycopolymer micelles was tested by specific binding using PNA lectins interaction with  $\beta$ -galactose moieties. The turbidity assay measures the changes in absorbance at a wavelength of 420 nm using UV/vis spectroscopy. With the binding to lectins the particles increase in size causing significant scattering, thus leading to a turbid solution. Figure 10 shows a typical turbidimetric assay curve.<sup>77</sup> The turbidity increases with conjugation time and plateaus after 10 min; this is a typical curve featuring a low epitope density of the diblock

copolymer used. A control experiment using ConA was carried out with the same polymeric ligand used with PNA. Results did not show any increased in turbidity as ConA is not specific toward  $\beta$ -galactose. Multivalent arrays displayed by the PS-*b*-P(GalEMA<sub>0.9-co</sub>-S<sub>0.1</sub>) glycopolymer allow high specific interactions between the  $\beta$ -galactose ligands on the polymers and PNA but virtually shows no interactions with ConA. This multivalent characteristic showed by the polyvalent glycopolymers was also observed earlier by Kiessling and co-workers.<sup>78,67</sup> UV difference spectra is another avenue to quantify lectin interaction with galactose.<sup>79</sup> The difference spectra were recorded, but due to the presence of styrene components in the micellar ligands, the overlap of the styrene absorbance at 290 nm with the lectin–ligand maximum at 286 nm resulted in a very small difference spectrum which could not be used for quantification.<sup>80</sup>

In addition to the turbidity test, online dynamic light scattering measurements were also conducted to monitor the size growth with conjugation time (Figures 11 and 12). The particle sizes increased steadily as more lectin was attached to the particles. Since PNA has four binding sides, intermicellar cross-linking occurred and led to an average hydrodynamic diameters of 300 nm after 30 min, which is a significant increase from the original micelle size of around 30 nm (Figure 12). The polydispersity of the particles increased dramatically when the lectin solution was added to the glycopolymer micelles; interestingly, it reduces to 0.08

after 15 min of conjugation time and rose back up again. The peanut agglutinin lectins have saturated the ligand particles after 20 min, resulting in an increase in polydispersity of the particles. The outcome of the light scattering experiment is dependent on the experimental procedure. This experiment was conducted by adding 200  $\mu$ L of the concentrated lectin stock solution (1 mg mL<sup>-1</sup>) to the polymer solution (0.1 mg mL<sup>-1</sup>). Preliminary screening conducted at a higher volume of lectin stock solution (400  $\mu$ L) when added to the same amount of polymer solution resulted in the more polydispersed particles when compared to the lower volume lectin stock solution used. Big aggregates were formed when the polymeric ligands were added into the concentrated lectin solution as reported previously.<sup>77</sup> This could be due to the concentration difference between the two solutions and also the disturbance of the micelles when it was added into the concentrated lectin solution, resulting in random aggregations and cross-linking.

Both experiments, UV–vis and scattering experiment, which were carried out using exactly the same procedure, gave slightly different results with UV–vis absorbance reaching a maximum after 10 min while the aggregate formation still continues looking at the results obtained from dynamic light scattering. This is not surprising considering that UV–vis only responds to a solution turning cloudy but can only distinguish to a very limited extent to different particle sizes.

Figures 11 and 12 and preliminary experiments allow us to conclude that the interaction of lectin with  $\beta$ -galactose on the particles was concentration and time dependent.<sup>35,81</sup>

**Morphology of PS-*b*-P(GalEMA<sub>0.9-co</sub>-S<sub>0.1</sub>) Honeycomb Structured Porous Films.** Honeycomb structured porous films with their hexagonal arrangement of pores can be obtained in a simple bottom-up procedure via the breath figure technique. The polymers are hereby dissolved in a highly volatile and water-immiscible solvent. With the fast evaporation of the solvent and the subsequent cooling of the solution surface, water droplets from the humid environment start condensing on the solution surface. The coalescence of the water droplets is prevented by the precipitation of polymer at the water–solution interface forming a solid envelop around the water droplets. The pores in the resulting film are therefore the result of empty water droplets, which act as templates during the formation process.<sup>23–25</sup> Earlier studies revealed that the formation of honeycomb structured porous films via breath figures using amphiphilic block copolymers leads to a nanosized substructure with hydrophilic pores and a hydrophobic surface.<sup>7,82,83</sup> Origin of this effect is the interaction of the amphiphilic polymer with the water droplets. While the interaction of the polymer with the water droplets can lead to interesting structures, it can also disrupt the film formation if the hydrophilic part of the

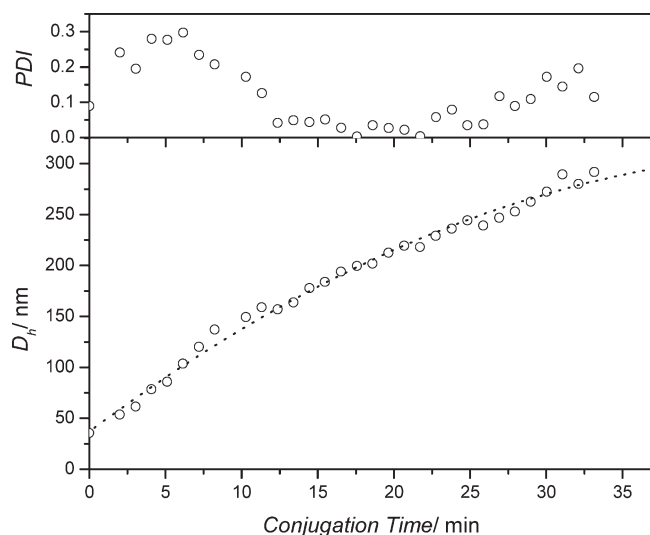


**Figure 12.** Dynamic light scattering measurements of the sizes evolution of conjugated PS-*b*-P(GalEMA<sub>0.9-co</sub>-S<sub>0.1</sub>) glycomicelles with peanut agglutinin and polydispersity indices vs conjugation times.

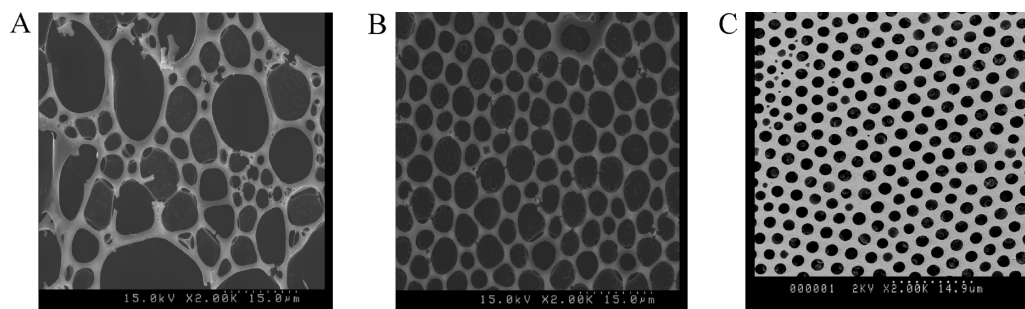


**Figure 13.** SEM images of polymeric porous films cast from PS-*b*-P(GalEMA<sub>0.9-co</sub>-S<sub>0.1</sub>) (A), a mixture of PS-*b*-P(GalEMA<sub>0.9-co</sub>-S<sub>0.1</sub>) and 6-arm star PS (MW 36 000 g mol<sup>-1</sup>) (B), and 6-arm star PS (MW 36 000 g mol<sup>-1</sup>) (C) in carbon disulfide.

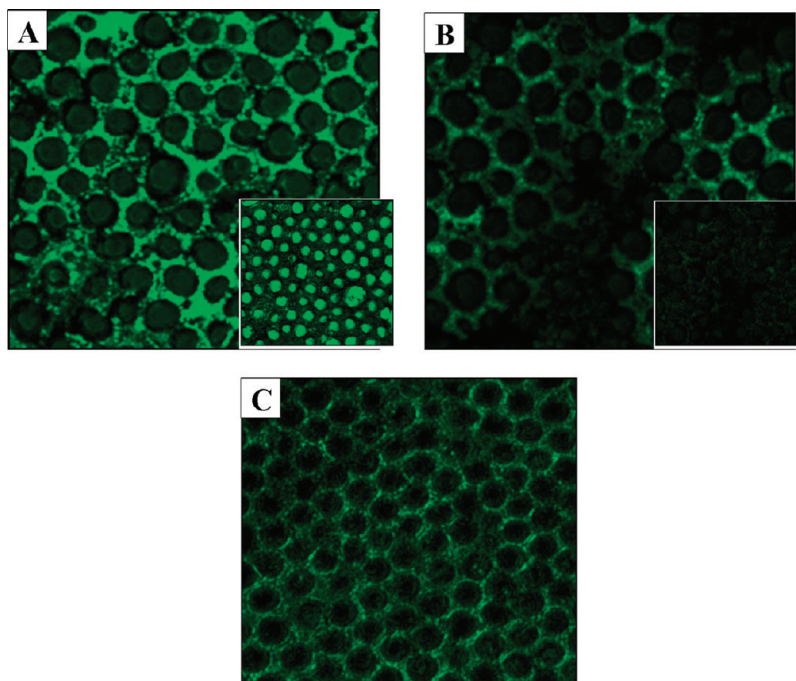


**Figure 14.** Confocal microscopy images of films cast from a polymers mixture of PS-*b*-P(GalEMA<sub>0.9-co</sub>-S<sub>0.1</sub>) and 6-arm star PS: (A) top section of film and (inset) cross section of film conjugated with FITC PNA and washed; (B) top section of film and (inset) cross section of film loaded with FITC ConA and washed; (C) top section of film cast from unfunctionalized 6-arm star PS only loaded with FITC PNA and washed.

polymer structure overpowers the precipitation process. The interference can indeed be observed here when using PS-*b*-P(GalEMA<sub>0.9-co</sub>-S<sub>0.1</sub>) for the formation of honeycomb structured porous films. As seen at Figure 13A, a highly irregular porous film was fabricated from PS-*b*-P(GalEMA<sub>0.9-co</sub>-S<sub>0.1</sub>). The amphiphilic block copolymer reduces the surface tensions of the water droplet; consequently, the water droplets are much more likely to coagulate with neighboring droplets, resulting in large disordered pores. In order to enhance pore regularity, the hydrophobic fraction in the polymer solution needs to be increased. This can be achieved by employing a block copolymer with a significantly larger polystyrene block or by mixing polystyrene homopolymer, preferably a polystyrene star polymer, into the solution. Therefore, 6-arm star PS (MW 36 000 g mol<sup>-1</sup>) was mixed with PS-*b*-P(GalEMA<sub>0.9-co</sub>-S<sub>0.1</sub>) (1:1 w/w) to prepare a solution in carbon disulfide (3 g L<sup>-1</sup>). The 6-arm star PS has previously been found to display a regular honeycomb patterned porous film.<sup>84</sup> Figure 13B shows an enhanced regularity of the hexagonal array. For comparison, the 6-arm star PS was used without the addition of PS-*b*-P(GalEMA<sub>0.9-co</sub>-S<sub>0.1</sub>) displaying a highly regular film (Figure 13C).

**PNA Binding on the Films.** To be able to visualize the conjugation of peanut agglutinin on the  $\beta$ -galactose functionalized porous films and to confirm a successful conjugation, two fluorescein isothiocyanate conjugated lectins, ConA and PNA, were employed. The films were immersed into a solution of protein and washed to remove any nonspecific binding. Fluorescence confocal microscopy was employed to locate the fluorescing proteins on the surface and in the pores. A point to note is that polystyrene is slightly fluorescent by itself due to the nature of the polymer.<sup>7</sup> Focusing on the surface of the films shows the increased fluorescence intensity of the films conjugated to PNA, indicating a strong binding between PNA (FITC) and  $\beta$ -galactose. (Figure 14A). The cross section through the pores however shows a significantly increased fluorescence intensity which confirms

earlier observations that the hydrophilic block—here glycopolymer—is mainly localized inside the pores, while the surface is enriched with polystyrene making these films usually highly hydrophobic. This demonstrates that the breath figure technique in combination with an amphiphilic block copolymer is an easy way to generate microarray for the selective immobilization of protein directly into the pores.

In contrast, no immobilization of FITC ConA was obtained (Figure 14B). Since ConA does not selectively conjugate to  $\beta$ -galactose, only weak fluorescence caused by the presence of polystyrene is observed. These results proved that the immobilization was highly site specific toward PNA, and the washing steps were efficient to remove any unbound protein. Further confirmation was carried out by loading FITC PNA on unfunctionalized 6-arms star PS porous film; the result indicates that only mild fluorescence could be observed from the image taken from the confocal microscope (Figure 14C), which is typical of untreated PS porous films when observed using the confocal microscope.<sup>85</sup>

## Conclusions

Biomaterials in the form of micelles and porous films were successfully developed via nitroxide SG1-mediated controlled free-radical polymerization of a methacryloyl galactose monomer. A block copolymer based on polystyrene-*block*-poly-(2-(2',3',4',6'-tetra-*O*-acetyl- $\beta$ -D-galactosyloxy)ethyl methacrylate-*co*-styrene) was deacetylated and self-assembled into micelles, and a “breath figure” technique was applied to develop glycopolymer-based porous films. The conditions for preparing PS-*b*-P(AcGalEMA-*co*-S) diblock copolymers were carefully investigated by varying the time for the preinitiation step. The control of AcGalEMA polymerization was achieved at 85 °C by using a low proportion of styrene as comonomer in all the NMP reactions. The biofunctionality of the  $\beta$ -galactose moieties on the porous films and micelles were screened using peanut agglutinin, a lectin specific for conjugating  $\beta$ -galactose. Results reveal that the polymerization conditions and the deacetylation process used



for synthesizing the diblock copolymers were safe enough to keep the biofunctionality of the materials intact. The location of the glycopolymer block of the diblock copolymer in the porous films was visualized using a fluorescent protein. Thanks to the galactose moieties on the surface of these materials, the micelles could possibly be used as drug delivery carrier to target liver hepatocytes in the body, which conjugate strongly to galactose. Pattern- ing of proteins onto the galactosylated porous films could be used as a screening device.

**Acknowledgment.** The authors thank the French-Australian Science and Technology Program (FAST) FR080066 for financial support and the Communauté d'Agglomération de Pau Pyrénées (CDAPP) for the foreign student scholarship to S. R. S. Ting and E. H. Min. L. Billon and M. Save thank Arkema for kindly providing SG1 and BlocBuilder alkoxyamine. The research exchange program in Pau, France would not be possible without the help and kind support from all the colleagues in IPREM/EPCP. S. R. S. Ting and E. H. Min thank A. Khouch and G. Clisson for the guidance on NMR and GPC analysis. The electron microscopy unit and the histology and microscopy unit in UNSW were also acknowledged. Lastly, S. R. S. Ting, E. H. Min, and M. H. Stenzel also thank I. Jacenyik and M. R. Whittaker for the management in CAMD.

**Supporting Information Available:** Synthesis and characterization of polystyrene macroinitiator (PS<sub>41</sub>-SG1); change transfer to solvent experiments for the polymerization of styrene with PS<sub>41</sub>-SG1 in dioxane; <sup>31</sup>P NMR of P(AcGalEMA<sub>0.9-co</sub>-S<sub>0.1</sub>) copolymer from experiment 1; <sup>1</sup>H NMR of PS<sub>180-b</sub>-P-(GalEMA<sub>0.9-co</sub>-S<sub>0.1</sub>) block copolymer from experiment 7; and TEM images of micelles derived from PS<sub>180-b</sub>-P-(GalEMA<sub>0.9-co</sub>-S<sub>0.1</sub>). This material is available free of charge via the Internet at <http://pubs.acs.org>.

**Note Added after ASAP Publication.** Minor revisions were made to the Supporting Information after the ASAP publication date of October 29, 2009. The correct version of the Supporting Information posted on November 9, 2009.

## References and Notes

- (1) Spain, S. G.; Gibson, M. I.; Cameron, N. R. *J. Polym. Sci., Part A: Polym. Chem.* **2007**, *45*, 2059–2072.
- (2) Ting, S. R. S.; Granville, A. M.; Quemener, D.; Davis, T. P.; Stenzel, M. H.; Barner-Kowollik, C. *Aust. J. Chem.* **2007**, *60*, 405–409.
- (3) Ting, S. R. S.; Gregory, A. M.; Stenzel, M. H. *Biomacromolecules* **2009**, *10*, 342–352.
- (4) Donovan, R. S.; Datti, A.; Baek, M.-G.; Wu, Q.; Sas, I. J.; Korczak, B.; Berger, E. G.; Roy, R.; Dennis, J. W. *Glycoconjugate J.* **1999**, *16*, 607–615.
- (5) Zhang, L.; Liu, W.; Lin, L.; Chen, D.; Stenzel, M. H. *Biomacromolecules* **2008**, *9*, 3321–3331.
- (6) Chen, G.; Tao, L.; Mantovani, G.; Geng, J.; Nystrom, D.; Haddleton, D. M. *Macromolecules* **2007**, *40*, 7513–7520.
- (7) Min, E.; Wong, K. H.; Stenzel, M. H. *Adv. Mater.* **2008**, *20*, 3550–3556.
- (8) Ting, S. R. S.; Nguyen, T. L. U.; Stenzel, M. H. *Macromol. Biosci.* **2009**, *9*, 211–220.
- (9) Pieters, R. J. *Org. Biomol. Chem.* **2009**, *7*, 2013–2025.
- (10) Dai, X.-H.; Dong, C.-M. *J. Polym. Sci., Part A: Polym. Chem.* **2008**, *46*, 817–829.
- (11) Dai, X.-H.; Dong, C.-M.; Yan, D. *J. Phys. Chem. B* **2008**, *112*, 3644–3652.
- (12) Deng, Z.; Li, S.; Jiang, X.; Narain, R. *Macromolecules* **2009**, *42*, 6393–6405.
- (13) Mateescu, A.; Ye, J.; Narain, R.; Vamvakaki, M. *Soft Matter* **2009**, *5*, 1621–1629.
- (14) Miyachi, A.; Dohi, H.; Neri, P.; Mori, H.; Uzawa, H.; Seto, Y.; Nishida, Y. *Biomacromolecules* **2009**, *10*, 1846–1853.
- (15) Nurmi, L.; Lindqvist, J.; Randev, R.; Syrett, J.; Haddleton, D. M. *Chem. Commun.* **2009**, 2727–2729.
- (16) Ruiz, C.; Sanchez-Chaves, M.; Cerrada, M. L.; Fernandez-Garcia, M. *J. Polym. Sci., Part A: Polym. Chem.* **2008**, *46*, 7238–7248.
- (17) Toyoshima, M.; Miura, Y. *J. Polym. Sci., Part A: Polym. Chem.* **2009**, *47*, 1412–1421.
- (18) Branderhorst, H. M.; Ruijtenbeek, R.; Liskamp, R. M. J.; Pieters, R. J. *ChemBioChem* **2008**, *9*, 1836–1844.
- (19) Kuil, J.; Branderhorst, H. M.; Pieters, R. J.; de Mol, N. J.; Liskamp, R. M. J. *Org. Biomol. Chem.* **2009**, *7*, 4088–4094.
- (20) Lee, R. T.; Lee, Y. C. *Glycoconjugate J.* **2001**, *17*, 543–551.
- (21) Roy, R. *Trends Glycosci. Glycotechnol.* **2003**, *15*, 291–310.
- (22) Billon, L.; Manguian, M.; Pellerin, V.; Joubert, M.; Eterradosi, O.; Garay, H. *Macromolecules* **2009**, *42*, 345–356.
- (23) Bunz, U. H. F. *Adv. Mater.* **2006**, *18*, 973–989.
- (24) Stenzel, M. H. *Aust. J. Chem.* **2002**, *55*, 239–243.
- (25) Widawski, G.; Rawiso, M.; Francois, B. *Nature* **1994**, *369*, 387–389.
- (26) Albertin, L.; Cameron, N. R. *Macromolecules* **2007**, *40*, 6082–6093.
- (27) Albertin, L.; Kohlert, C.; Stenzel, M.; Foster, L. J. R.; Davis, T. P. *Biomacromolecules* **2004**, *5*, 255–260.
- (28) Albertin, L.; Stenzel, M.; Barner-Kowollik, C.; Foster, L. J. R.; Davis, T. P. *Macromolecules* **2004**, *37*, 7530–7537.
- (29) Albertin, L.; Stenzel, M. H.; Barner-Kowollik, C.; Foster, L. J. R.; Davis, T. P. *Macromolecules* **2005**, *38*, 9075–9084.
- (30) Albertin, L.; Stenzel, M. H.; Barner-Kowollik, C.; Foster, L. J. R.; Davis, T. P. *Polymer* **2005**, *46*, 2831–2835.
- (31) Deng, Z.; Ahmed, M.; Narain, R. *J. Polym. Sci., Part A: Polym. Chem.* **2009**, *47*, 614–627.
- (32) Ohno, K.; Izu, Y.; Yamamoto, T.; Fukuda, T. *Macromol. Chem. Phys.* **1999**, *200*, 1619–1625.
- (33) Ohno, K.; Tsujii, Y.; Fukuda, T. *J. Polym. Sci., Part A: Polym. Chem.* **1998**, *36*, 2473–2481.
- (34) Ohno, K.; Tsujii, Y.; Miyamoto, T.; Fukuda, T.; Goto, M.; Kobayashi, K.; Akaike, T. *Macromolecules* **1998**, *31*, 1064–1069.
- (35) Ladmiral, V.; Mantovani, G.; Clarkson, G. J.; Cauet, S.; Irwin, J. L.; Haddleton, D. M. *J. Am. Chem. Soc.* **2006**, *128*, 4823–4830.
- (36) Wang, Y.; Kiick, K. L. *J. Am. Chem. Soc.* **2005**, *127*, 16392–16393.
- (37) Xiao, N.-Y.; Li, A.-L.; Liang, H.; Lu, J. *Macromolecules* **2008**, *41*, 2374–2380.
- (38) Loykulant, S.; Hirao, A. *Macromolecules* **2000**, *33*, 4757–4764.
- (39) Murphy, J. J.; Furusho, H.; Paton, R. M.; Nomura, K. *Chem.—Eur. J.* **2007**, *13*, 8985–8997.
- (40) Ohno, K.; Fukuda, T.; Kitano, H. *Macromol. Chem. Phys.* **1998**, *199*, 2193–2197.
- (41) Götz, H.; Harth, E.; Schiller, S. M.; Frank, C. W.; Knoll, W.; Hawker, C. J. *J. Polym. Sci., Part A: Polym. Chem.* **2002**, *40*, 3379–3391.
- (42) Chen, Y.; Wulff, G. *Macromol. Chem. Phys.* **2001**, *202*, 3273–3278.
- (43) Chen, Y.; Wulff, G. *Macromol. Chem. Phys.* **2001**, *202*, 3426–3431.
- (44) Narumi, A.; Satoh, T.; Kaga, H.; Kakuchi, T. *Macromolecules* **2002**, *35*, 699–705.
- (45) Narumi, A.; Matsuda, T.; Kaga, H.; Satoh, T.; Kakuchi, T. *Polymer* **2002**, *43*, 4835–4840.
- (46) Meng, J. Q.; Du, F. S.; Liu, Y. S.; Li, Z. C. *J. Polym. Sci., Part A: Polym. Chem.* **2005**, *43*, 752–762.
- (47) Muthukrishnan, S.; Erhard, D. P.; Mori, H.; Muller, A. H. E. *Macromolecules* **2006**, *39*, 2743–2750.
- (48) Muthukrishnan, S.; Jutz, G.; Andre, A.; Mori, H.; Muller, A. H. E. *Macromolecules* **2005**, *38*, 9–18.
- (49) Vazquez-Dorbatt, V.; Maynard, H. D. *Biomacromolecules* **2006**, *7*, 2297–2302.
- (50) Al-Bagoury, M.; Buchholz, K.; Yaacoub, E. J. *Polym. Adv. Technol.* **2007**, *18*, 313–322.
- (51) Albertin, L.; Stenzel, M. H.; Barner-Kowollik, C.; Davis, T. P. *Polymer* **2006**, *47*, 1011–1019.
- (52) Bernard, J.; Hao, X. J.; Davis, T. P.; Barner-Kowollik, C.; Stenzel, M. H. *Biomacromolecules* **2006**, *7*, 232–238.
- (53) Lowe, A. B.; Sumerlin, B. S.; McCormick, C. L. *Polymer* **2003**, *44*, 6761–6765.
- (54) Ozyurek, Z.; Komber, H.; Gramm, S.; Schmaljohann, D.; Muller, A. H. E.; Voit, B. *Macromol. Chem. Phys.* **2007**, *208*, 1035–1049.
- (55) Roy, D.; Cambre, J. N.; Sumerlin, B. S. *Chem. Commun.* **2008**, 2477–2479.
- (56) Zhang, L.; Bernard, J.; Davis, T. P.; Barner-Kowollik, C.; Stenzel, M. H. *Macromol. Rapid Commun.* **2008**, *29*, 123–129.
- (57) Pearson, S.; Allen, N.; Stenzel, M. H. *J. Polym. Sci., Part A: Polym. Chem.* **2009**, *47*, 1706–1723.

- (58) Chang, C.-W.; Bays, E.; Tao, L.; Alconcel, S. N. S.; Maynard, H. D. *Chem. Commun.* **2009**, 3580–3582.
- (59) Damiani, E.; Greci, L.; Hrelia, P. *Free Radical Biol. Med.* **2000**, *28*, 330–336.
- (60) Hahn, S. M.; Krishna, M. C.; DeLuca, A. M.; Coffin, D.; Mitchell, J. B. *Free Radical Biol. Med.* **2000**, *28*, 953–958.
- (61) Dire, C.; Belleney, J.; Nicolas, J.; Bertin, D.; Magnet, S.; Charleux, B. *J. Polym. Sci., Part A: Polym. Chem.* **2008**, *46*, 6333–6345.
- (62) Charleux, B.; Nicolas, J.; Guerret, O. *Macromolecules* **2005**, *38*, 5485–5492.
- (63) Nicolas, J.; Dire, C.; Mueller, L.; Belleney, J.; Charleux, B.; Marque, S. R. A.; Bertin, D.; Magnet, S.; Couvreur, L. *Macromolecules* **2006**, *39*, 8274–8282.
- (64) Nicolas, J.; Mueller, L.; Dire, C.; Matyjaszewski, K.; Charleux, B. *Macromolecules* **2009**, *42*, 4470–4478.
- (65) Dire, C.; Charleux, B.; Magnet, S.; Couvreur, L. *Macromolecules* **2007**, *40*, 1897–1903.
- (66) Nygard, A.; Davis, T. P.; Barner-Kowollik, C.; Stenzel, M. H. *Aust. J. Chem.* **2005**, *58*, 595–599.
- (67) Stenzel-Rosenbaum, M.; Davis, T. P.; Chen, V.; Fane, A. G. *J. Polym. Sci., Part A: Polym. Chem.* **2001**, *39*, 2777–2783.
- (68) Nebhani, L.; Sinnwell, S.; Inglis, A. J.; Stenzel, M. H.; Barner-Kowollik, C.; Barner, L. *Macromol. Rapid Commun.* **2008**, *29*, 1431–1437.
- (69) Yang, J.; Goto, M.; Ise, H.; Cho, C.-S.; Akaike, T. *Biomaterials* **2001**, *23*, 471–479.
- (70) Ambrosi, M.; Batsanov, A. S.; Cameron, N. R.; Davis, B. G.; Howard, J. A. K.; Hunter, R. J. *Chem. Soc., Perkin Trans. 1* **2002**, 45–52.
- (71) Spain, S. G.; Albertin, L.; Cameron, N. R. *Chem. Commun.* **2006**, 4198–4200.
- (72) Benoit, D.; Grimaldi, S.; Robin, S.; Finet, J.-P.; Tordo, P.; Gnanou, Y. *J. Am. Chem. Soc.* **2000**, *122*, 5929–5939.
- (73) Chauvin, F.; Dufils, P.-E.; Gimes, D.; Guillauneuf, Y.; Marque, S. R. A.; Tordo, P.; Bertin, D. *Macromolecules* **2006**, *39*, 5238–5250.
- (74) Theodoly, O.; Jacquin, M.; Muller, P.; Chhun, S. *Langmuir* **2009**, *25*, 781–793.
- (75) Khan, T. N.; Mobbs, R. H.; Price, C.; Quintana, J. R.; Stubbersfield, R. B. *Eur. Polym. J.* **1987**, *23*, 191–194.
- (76) Chen, W.; Zhu, M.; Song, S.; Sun, B.; Chen, Y.; Adler, H.-J. P. *Macromol. Mater. Eng.* **2005**, *290*, 669–674.
- (77) Chen, G.; Amajjahe, S.; Stenzel, M. H. *Chem. Commun* **2009**, 1198–1200.
- (78) Mortell, K. H.; Weatherman, R. V.; Kiessling, L. L. *J. Am. Chem. Soc.* **1996**, *118*, 2297–2298.
- (79) Neurohr, K. J.; Bundle, D. R.; Young, N. M.; Mantsch, H. H. *Eur. J. Biochem.* **1982**, *123*, 305–310.
- (80) Li, T.; Zhou, C.; Jiang, M. *Polym. Bull.* **1991**, *25*, 211–216.
- (81) Cairo, C. W.; Gestwicki, J. E.; Kanai, M.; Kiessling, L. L. *J. Am. Chem. Soc.* **2002**, *124*, 1615–1619.
- (82) Stenzel, M. H.; Barner-Kowollik, C.; Davis, T. P. *J. Polym. Sci., Part A: Polym. Chem.* **2006**, *44*, 2363–2375.
- (83) Wong, K. H.; Davis, T. P.; Barner-Kowollik, C.; Stenzel, M. H. *Polymer* **2007**, *48*, 4950–4965.
- (84) Stenzel-Rosenbaum, M. H.; Davis, T. P.; Fane, A. G.; Chen, V. *Angew. Chem., Int. Ed.* **2001**, *40*, 3428–3432.
- (85) Hernandez-Guerrero, M.; Min, E.; Barner-Kowollik, C.; Mueller, A. H. E.; Stenzel, M. H. *J. Mater. Chem.* **2008**, *18*, 4718–4730.